WELL LOG AND CORE-DERIVED RESERVOIR PROPERTIES OF BARNETT SHALE OF FORT WORTH BASIN

by

MELANIE YBARRA

Presented to the Faculty of the Graduate School of
The University of Texas at Arlington in Partial Fulfillment
of the Requirements
for the Degree of

MASTER OF SCIENCE IN GEOLOGY

THE UNIVERSITY OF TEXAS AT ARLINGTON

December 2014

Acknowledgements

I would like to express my gratitude to my advisor, Dr. Max Hu, for his support of my thesis study and research. His sound judgment, advice, and knowledge has helped guide me through this work.

I would also like to thank Daniel Ortuno and Dr. Qilong Fu from BEG for providing me with digital well log data for the study well. Drillinginfo has provided myself and our research team at UTA with access to their site for data gathering. Bill Knights, Gary Paisley, and Jim Davidson with Netherland, Sewell, and Associates have helped guide me for years, pointing me to great research, and answering my numerous questions.

Lastly, I would like to thank my family. My husband, Khoji Ybarra, has been my rock through many years of school, work, and family. I am forever grateful.

November 30, 2014

Abstract

WELL LOG AND CORE-DERIVED RESERVOIR

PROPERTIES OF BARNETT SHALE OF

FORT WORTH BASIN

Melanie Ybarra, M.S.

The University of Texas at Arlington, 2014

Supervising Professor: Qinhong Hu

Wireline tools and log analysis methods were not designed for unconventional reservoirs. As a result, hydrocarbon assessment for shale source rock plays have significant uncertainties. This study focuses on petrophysical interpretation uncertainty from a single historic Barnett Shale well TP Sims #2 of Wise County, TX. The Barnett Shale is one of the major source rock plays in the United States. The large body of research and information from the well-drilled Barnett Shale provides a good opportunity to understand and adjust OGIP modeling approaches from volumetric analysis to well performance data. Several factors unique to shale source rocks such as TOC and pyrite have been incorporated into wireline log interpretation using core-derived correlations. Key petrophysical parameters that are estimated from well logs calibrated to core data include: mineral volumes, porosity, net pay, and water saturation. Volumetric OGIP calculations from a range of well log analysis results that have been calibrated to core for TP Sims #2 are compared with EUR data. The resulting recovery factors are larger than expected which may mean that volumetric OGIP remains deficient for resource assessment of shale plays.

Table of Contents

List of Illustrations

List of Tables

Chapter 1

Introduction

Resource Assessment Challenges of Unconventional Shale Gas Reservoirs

The term unconventional reservoir refers to a reservoir that does not owe its existence to the buoyancy of gas in water (Schmoker 2002). Shale source rock plays are unconventional reservoirs that have become important economic resources in the past decades with the advent and improvement of horizontal drilling and hydraulic fracturing. Since most reservoir characterization techniques have been developed for conventional reservoirs, there can be large uncertainties with quantifying original gas-in-place (OGIP) for unconventional reservoirs.

The two main ways to estimate OGIP are from established production history profiles and volumetric assessment. Barring production problems, accurate estimates of recoverable gas-in-place from volumetric analyses would closely align with the produced gas volumes (i.e. both methods would predict similar OGIP). However, using geologic and petrophysical data for volumetric assessment of OGIP can be difficult for shale source rocks because they contain organic matter and pyrite that can complicate the interpretation of reservoir properties.

Production-derived estimates of OGIP can be made with well performance data and recovery factors, and therefore avoid the use of geologic and petrophysical data. Estimates of ultimate recovery (EUR) can be forecasted from well production profiles. If the recovery factor is known for a reservoir, the OGIP can be estimated because the EUR to OGIP ratio is the recovery factor. However, the EUR/RF method of deriving OGIP requires an established production history and known recovery factor, and lacks applicability to resource assessment in early stages of exploration. There is a need to accurately quantify and calibrate OGIP volumetric estimates for shale reservoirs based on geologic and petrophysical data.

Previous work in resource assessment of unconventional gas fields has typically found that volumetrically-derived recoverable gas-in-place estimates are generated from large total gas-in-place multiplied by a low recovery factor (Schmoker 2002). Alternatively, assessment methods that focus on well performance are empirical forecasts of OGIP (Schmoker 2002). EUR based on

production profiles has been found to be approximately 204 bcf/section for wells targeting Barnett Shale of Fort Worth Basin (Jarvie et al., 2007). Total recoverable gas-in-place volumes of 26 trillion cubic feet (tcf) have been estimated by the United States Geological Survey (Pollastro et al., 2007).

The goals of this study are to explore reservoir characteristics of Barnett Shale from well log and core analysis, and to compare results from volumetric analysis to well performance derived analysis of OGIP. Volumetric methods use geologic and petrophysical data to quantify reservoir characteristics. Mineralogy, porosity water saturation, gas adsorbtion, net pay and permeability are important factors for reservoir characterization of Barnett Shale that are discussed in detail. Methods for calculating reservoir properties from well logs that can be calibrated to core measurements are explored. Factors unique to shale source rock plays, such as kerogen and ultra-low permeability, and their impact on the volumetric analysis will be examined, as well as uncertainty associated with the reservoir characteristics of shale plays. The research herein focuses on calculating recoverable OGIP of Barnett Shale from volumetric assessment and comparing results to volumes from EUR analysis. The petrophysical properties as interpreted from core study and well log interpretation are used to obtain estimates of effective pore space, gas saturation, and net reservoir thickness. Gas property data are used to calculate gas expansion factor. Uncertainty with porosity and reservoir cutoff criteria are used to define a range of volumetrically derived OGIP

Key components to quantifying the amount of original gas-in-place within a reservoir are porosity, net reservoir rock, and hydrocarbon saturation. Shales are characterized by ultra low permeability. However, hydraulic fracturing of shale reservoirs creates a highly variable two component permeability system. Organic rich shale plays contain varying amounts and types of kerogen. Kerogen is decomposed solid organic matter that can often have well-connected gas-filled pore spaces. The organic solids will have an effect on the wireline log responses and reservoir properties. Electrical measurements of formation resistivity (used for estimating water saturation) will be affected by rock, liquid hydrocarbon, and gas hydrocarbons, and also by solid

immobile hydrocarbons (kerogen). Also, nuclear tools designed for estimating porosity of the formation will be affected by the presence of solid organic material in the formation. Quantifying the solid organic matter and understanding the type of organic matter will affect the wireline tool analysis, thus affecting the OGIP volumetric estimates of the shale source rock reservoir.

Typical methods designed for estimating porosity are analysis of wireline well log data and laboratory analysis of cores. The wireline porosity of a conventional reservoir with known lithology is a relatively simple calculation. However, the presence of organic material in a shale source rock play fills pore space. This complicates the porosity estimation process as it affects the wireline tool reading.

Drilling direction of lateral wells is determined by the natural fracture orientation. Identifying the orientation of a natural fracture system within a source rock play can aid in making better drilling direction decisions so as to maximize the connectivity and ultimate flow of hydrocarbons to the wellbore. If a reservoir is naturally fractured, drilling orientation can exploit the fracture system by increasing the effective net rock that will contribute to production. Wells drilled orthogonal to the natural fracture network should have greater OGIP estimates than a similar well at a different orientation to the fracture system.

Study Objective

A review of literature reveals a wide array of geologic factors that affect gas-in-place estimates of unconventional shale gas reservoirs. An integrated petrophysical and geologic modeling approach that results in meaningful volumetric estimates is lacking. The objective of this study is to identify and quantify key factors for shale gas resource assessment in the Barnett Shale play. Laboratory core measurements and well log data from a gas-producing Barnett Shale well were used to calibrate a petrophysical model of key rock properties. Specific objectives are:

(1) To develop methods to predict mineralogy, TOC, porosity, and water saturation from well log measurements that is tied to the core measurements
(2) To use well log-derived analysis to volumetrically estimates OGIP
(3) To compare results of OGIP from volumetrics to well performance estimates

Overview of Thesis Organization

The remainder of Chapter 1 is devoted to introducing background information, including the geologic setting of Barnett Shale, Newark Gas Field history, and geologic characteristics of shale source rocks. Chapter 2 contains the study's methodology including the steps used to calculate volumetrics from well log and core data, and performance-derived estimates of OGIP. The results are presented in Chapter 3. Chapter 4 will conclude with discussion of the significance of the results and future study recommendations.

Geologic Setting of Barnett Shale in Fort Worth Basin

Gas shales are source rocks that typically cover large areas and are often naturally fractured. When assessing the hydrocarbon potential of these unconventional accumulations, depositional setting, burial history, hydrocarbon generation, and structural evolution are important to understand.

Structural Evolution and Stratigraphy of the Fort Worth Basin

The Fort Worth Basin is a shallow, north-south elongated trough covering approximately 15,000 mi^2 in north-central Texas (Pollastro et al., 2007). It is one of several Paleozoic foreland basins formed by the Ouachita thrust front (Pennsylvanian age). The Ouachita thrust front was the result of collisional tectonics during the formation of Pangea (Pollastro et al., 2007). Other basins in this trend include Black Warrior, Arkoma, Kerr, Val Verde, and Marfa basins (Pollastro et al., 2007).

The basin is northward deepening and the axis trends roughly parallel to the Ouachita front (Figure 1-1). The eastern boundary generally follows the Ouachita front. The northern margin is fault-bounded by Pennsylvanian-age Red River and Muenster arches. These basement uplifts are part of the northwest-striking Amarillo-Wichita uplift trend which has been interpreted to be the result of basement faults reactivated during Ouachita compression (Pollastro et al., 2007). To the west, the basin shallows and the boundary trends north-south along the eastern shelf of the Permian Basin, the Bend arch, and the Concho platform. The domal Llano uplift, which exposes Precambrian and Paleozoic rocks, bounds the basin to the south.

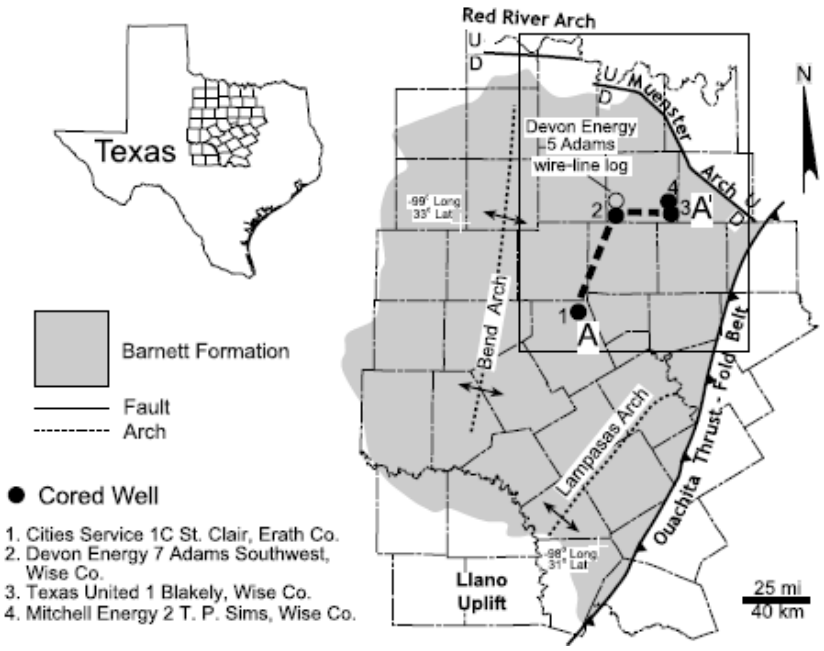

Figure 1-1 General structural features of Fort Worth Basin (Montgomery et al., 2005)

Paleogeographic reconstructions as shown in Figure 1-2 suggest that during the Mississippian, the Fort Worth Basin area occupied a narrow inland seaway between the rapidly approaching continents of Laurussia and Gondwana (Loucks and Ruppel, 2007). The Mississippian Interior seaway was bounded to the west by a broad shallow-water carbonate shelf (Chappel Shelf) and on the east by Caballos-Arkansas Island Chain. It extended along most of the southern and southeastern margins of the Laurussian paleocontinent. The Fort Worth basin formed as a foreland basin on the edge of the Laurussian paleocontinent.

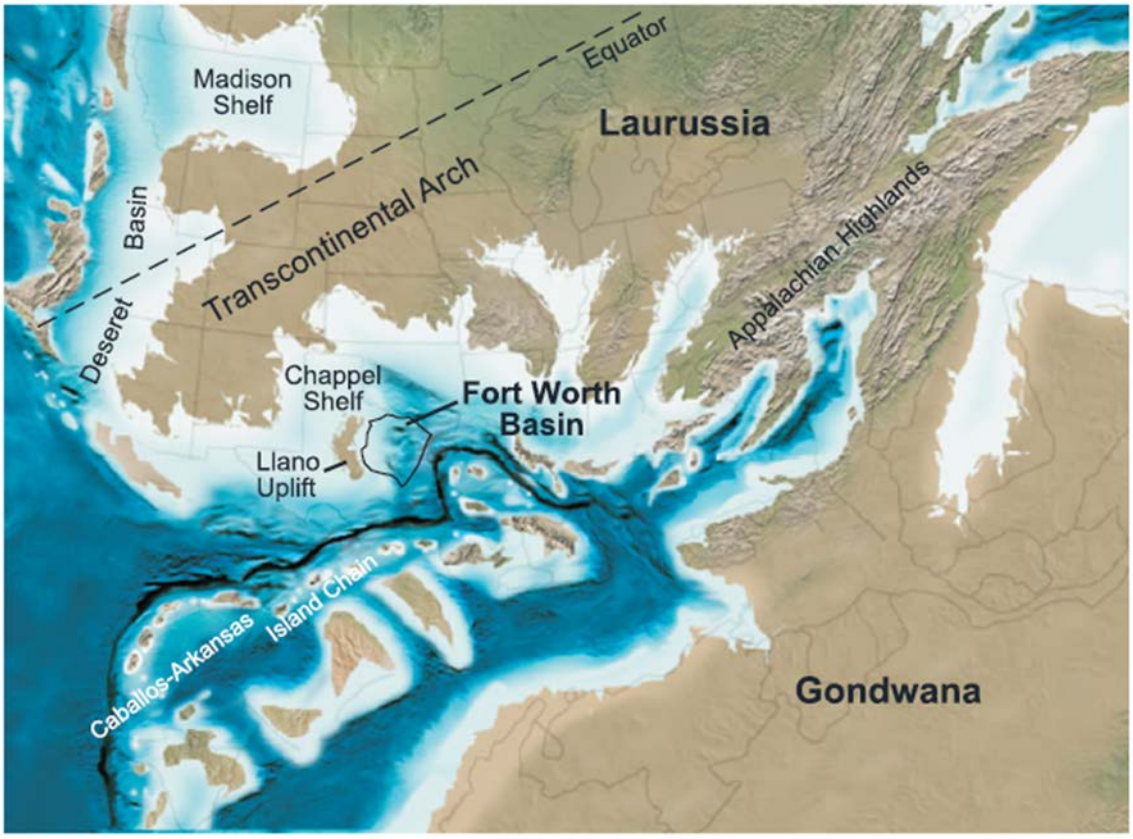

Figure 1-2 Late Mississippian (325 Ma) paleogeography (Loucks and Ruppel, 2007)

Based on sediment thickness, the deepest part of the basin was to the northeast. Approximately 12,000' of basin fill is preserved in the northeast corner adjacent to the Muenster arch. About 4000'-5000' of Ordovician to Mississippian carbonates and shales are overlain by 6000'-7000' of Pennsylvanian clastics and carbonates. In the eastern portion there is a thin layer of Cretaceous rocks; however, no Tertiary rocks are present (Loucks and Ruppel 2007).

Present day Mississippian age Barnett Shale of Fort Worth Basin occurs in 38 counties in north-central Texas as well as nearby basins (Jarvie et al., 2007). Age-equivalent shales are present along the eastern flank of the Ouachita thrust (Jarvie et al., 2007). Erosion has made the Barnett absent over the Muenster arch, a Pennsylvanian-age horst block (Loucks and Ruppel 2007).

Figure 1-3 is a generalized cross section and stratigraphic column of Fort Worth Basin. Devonian and Permian sections are notably absent as the Mississipian Barnett Shale

unconformably overlies Ordovician Viola Limestone in the study area of the eastern part of the Fort Worth basin. The Barnett Shale is conformably overlain by Pennsylvanian Marble Falls Limestone. The Barnett Shale is therefore overlain and underlain by impermeable limestones. In the eastern part of the basin, Forestburg limestone separates upper and lower Barnett Shale (Loucks and Ruppel 2007). This limestone is also the thickest on the southwest side of the Muenster arch, again indicating large accommodation space to the northeast. The depth of Barnett Shale is approximately 6500' - 8500' and thickness varies from 10' to over 1000' (Pollastro et al., 2007).

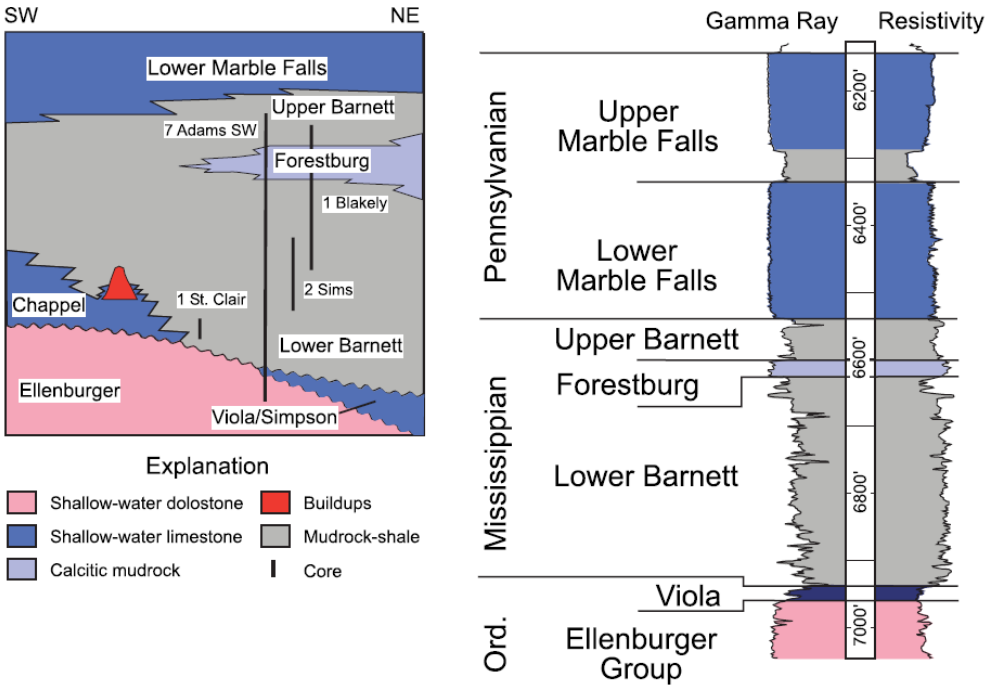

Figure 1-3 Ordovician to Pennsylvanian stratigraphy across Fort Worth Basin showing TP Sims #2 penetration

Depositional Environment of Barnett Formation

Barnett strata were deposited in a deep water foreland basin that had poor circulation with the open ocean (Loucks and Ruppel, 2007). Barnett sediments clearly indicate a deposition below the storm-wave base, as well as beneath an oxygen-minimum zone. Much of the organic matter deposited was preserved because bottom waters were euxinic, thus making it a rich

source rock. The major components are clay- to silt-sized particles containing abundant pyrite and phosphate (Hickey and Henk 2007). The main lithofacies that have been described from core and outcrop study are laminated argillaceous mudstone, laminated siliceous lime mudstone (marl), and skeletal, argillaceous lime packstone (Loucks and Ruppel, 2007). Sediment transport is thought to occur via mud plumes, turbidites, and debris flows from shelf or oxygenated slope deposits (Loucks and Ruppel, 2007). Other main lithofacies identified in core study include organic rich black shale, fossiliferous shale, dolomite rhomb shale, dolomitic shale, phosphatic shale, and concretionary carbonate (Hickey and Henk 2007). Extensive early microbial alteration of abundant organic matter helped to develop these lithofacies (Hickey and Henk 2007). Sedimentation is believed to occur consistently over an estimated 25-m.y. period.

Barnett-Paleozoic Total Petroleum System

The Barnett-Paleozoic total petroleum system (TPS) of the Fort Worth Basin refers to thermally mature Barnett Shale that has generated large volumes of hydrocarbons contained both within the Barnett Shale and those which have been expelled and distributed among numerous conventional clastic- and carbonate-rock reservoirs of Paleozoic age (Pollastro 2007). The Barnett Shale is one of the most prolific shale gas-producing formation and is also the primary source rock for oil and gas produced from other Paleozoic reservoir rocks within the basin.

Newark East Gas Field

Barnett Shale gas wells are designated as the Newark East Gas Field by the Texas Railroad Commission (TRC). The field was discovered in 1981 by Mitchell Energy. Initial gas wells had low production rates but Mitchell Energy's persistence in the Barnett Shale eventually paid off after drilling technologies in tight reservoirs improved (Martineau 2007). The Barnett Shale became the first shale play to be developed extensively and altered the US natural-gas supply significantly (Browning 2013). Devon Energy acquired Mitchell Energy in 2002, and has continued to improve drilling and completion technologies for increased production within the Barnett Shale. Nearly 18,000 wells have been drilled as December of 2013 (Nicot et al., EST, 2014).

Geologic Characteristics of Shale Gas Systems

While certain geologic aspects of hydrocarbon systems are the same for both shale gas systems and conventional reservoirs, there are several important characteristics unique to shale gas systems. As with conventional reservoirs, deposition, maturation, and preservation must have occurred. However, shale gas systems differ in that they are simultaneously the source, trap, and reservoir. Figure 1-4 is a diagram highlighting key differences in various reservoir types. Geologic factors such as mineralogy, organic richness, maturity, and gas adsorption potential are important when describing the shale gas reservoir characteristics. Natural fracturing is often a main driver for gas production and storage as significant quantities of gas are stored in large fracture-connected pore spaces.

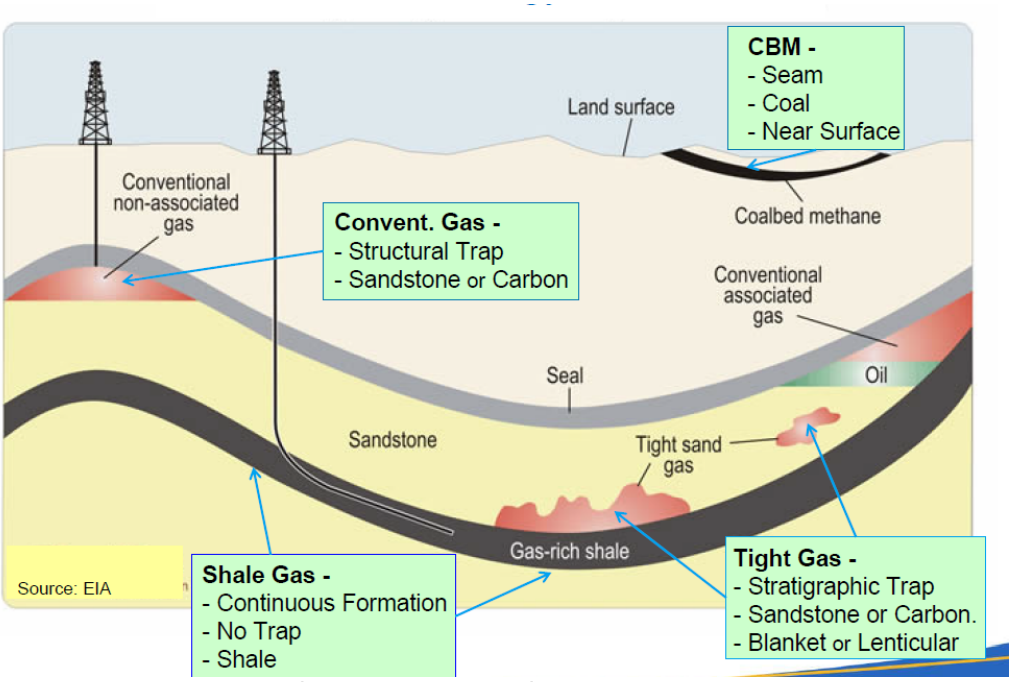

Figure 1-4 Gas petroleum systems

Kerogen

Kerogen is a mixture of organic compounds found in sedimentary rocks. It is insoluble in normal organic solvents and has high molecular weights (Tissot and Welte, 1978). The soluble portion of organic compounds found in organic matter is bitumen. When kerogen is preserved in sedimentary rocks and then exposed to temperature and pressure in the oil (50-150 deg C) or

gas (150-200 deg C) windows, petroleum is generated from the thermal degradation of kerogen. This process, known as thermal maturation, occurs with sedimentation and subsidence. As thermal maturation proceeds, kerogen is subjected to diagenesis, catagenesis and finally metagenesis (Tissot and Welte, 1978). Kerogen can be classified according to its source material. Table 1-1 shows the various types of kerogen defined by geochemical characteristics, and Table 1-2 shows kerogen types and their hydrocarbon source potential (PA DCNR, 2014). Barnett Shale lies in the thermal gas-generation window and is classified as a type II kerogen (Jarvie et al., 2004). A chemical analysis method used for classifying organic matter type is by measuring the relative abundance of elemental carbon (C), oxygen (O), and hydrogen (H) and plotting the H/C and O/C on a Van Krevelen diagram. A Van Krevelen diagram shows kerogen evolution pathways for several kerogen types from diagenesis to metagenesis (Tissot and Welte, 1978). Figure 1-5 displays the kerogen evolution pathways for three main kerogen types on a Van Krevelen plot. Common laboratory pyrolysis techniques estimate the hydrogen index from the amount of pyrolyzable hydrocarbon, S_2, divided by the total organic carbon (TOC), and the oxygen index from the carbon dioxide produced during pyrolysis, S_3, divided by TOC (Tissot and Welte, 1978). These laboratory measurements are used to determine hydrocarbon potential.

.

Table 1-1 Kerogen type, hydrogen content, and origin

Kerogen Type	Maceral group	Origin	Hydrogen content
I and II	Exinite	Spores, planktonic debris	Hydrogen-rich
III	Vitrinite	Land plants	Hydrogen-poor
IV	Inertinite	Fossil charcoal, fungal remains	Hydrogen-poor

Table 1-2 Properties of different kerogen types

Quality of Organic Matter*				
Kerogen Type	**Kerogen Composition**	**Hydrogen Index (HI) (mg HC/g TOC)**	**S2/S3**	**Main Product Expelled at Peak Maturity**
I	amorphous/alginite	>600	>15	oil
II	exinite	300-600	10-15	oil
II/III	exinite/vitrinite	200-300	5-10	mixed oil and gas
III	vitrinite	50-200	1-5	gas
IV	inertinite	<50	<1	none

** Approximate ranges based on thermally immature source rocks*

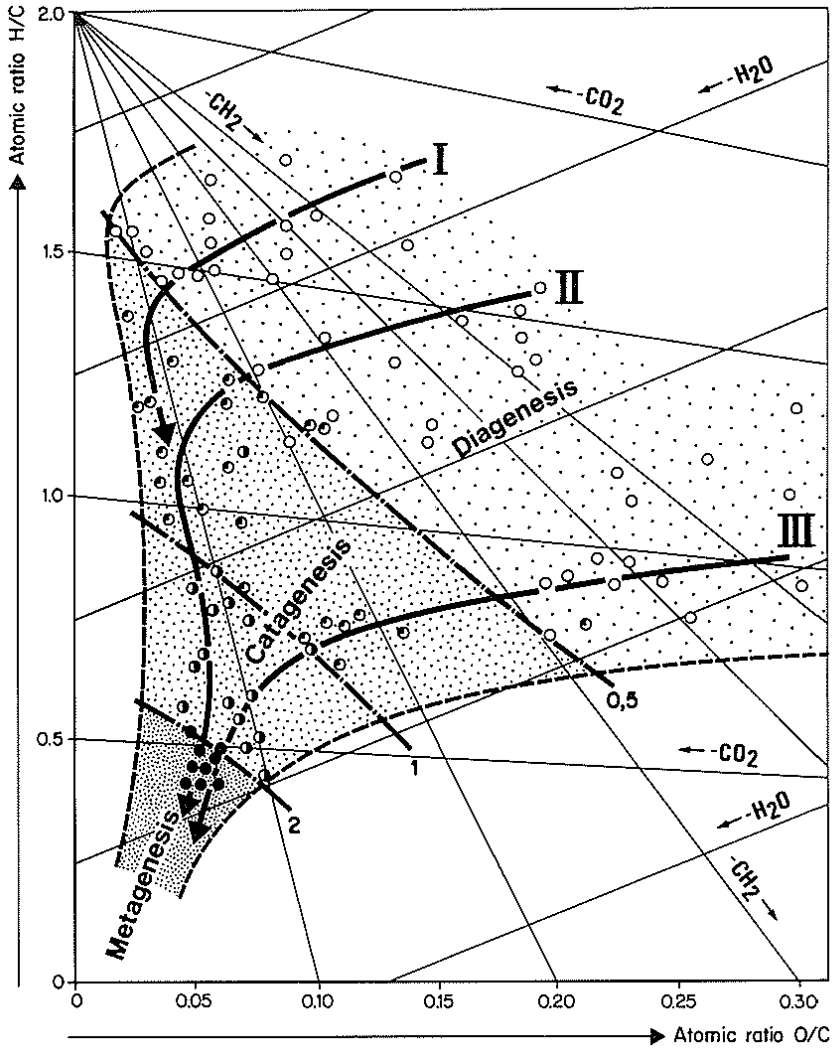

Figure 1-5 Van Krevelen diagram with corresponding kerogen types and approximate vitrinite reflectance

Total Organic Carbon

Total organic carbon in the form of kerogen has historically been measured in laboratories to assess the quality of source rocks. Estimates are obtained by heating the sample in a furnace and combusting the carbon to carbon dioxide at 600 deg C (TAMU, 2014). The amount of carbon liberated is related to the organic carbon content in the rock. Corrections for carbon from inorganic minerals, mostly carbonates, are necessary to determine the organic

carbon content. Since the other elements associated with kerogen are excluded, the resulting weight fraction of organic carbon is less than the weight fraction of total kerogen.

Thermal Maturity and Vitrinite Reflectance

A maceral is a component of organic material analogous to minerals of rocks. Macerals are considered to be dehydrogenated plant fragments. Inertinite, vitrinite and liptinite are types of macerals defined by their organic source and identified by petrographers according to their grayness in reflected light (Tissot and Welte, 1978). In particular, vitrinite is thought to have derived from higher plant tissues and passed to the gelification stage (Tissot and Welte, 1978). A commonly used approach to the measurement of organic maturity is by vitrinite reflectance. Vitrinite reflectance is used to identify the maximum paleotemperature for sediment in a basin and is a thermal maturity indicator.

Thermal maturity is a key factor for understanding where and what type of hydrocarbons can be found within a shale play. Vitrinite reflectance was first widely used in the coal industry as a thermal maturity indicator, and has more recently been used as a tool to study organic matter from kerogen. Vitrinite reflectance can be obtained either from visual methods or chemical analysis using laboratory RockEval procedures. Visual analysis includes petrographic microscopic examination of vitrinite from rock mounts and recordings of reflectivity of particles via a photomultiplier (Jarvie et al., 2007). The onset of the oil window, the paleotemperature range in which oil generation occurs, correlates to vitrinite reflectance of 0.5-0.6% and terminates at 0.85-1.1%. The onset of gas generation correlates with 1.0-1.3% and ends at about 3.0%. RockEval is a common source rock laboratory protocol often used to obtain thermal maturity and kerogen type data needed to evaluate source rocks. RockEval pyrolysis methods consist of heating a small sample (~100 mg) in an inert oven to determine free hydrocarbons, hydrogen- and oxygen-containing compounds (CO2) that volatilized during the “cracking” of kerogen. A correlation of maximum temperature achieved during RockEval kerogen cracking, Tmax, to vitrinite reflectance has been found for Barnett Shale samples (Jarvie et al., 2001). This correlation is particularly useful in gaining thermal maturity information in marine shale environments where there is a lack

of vitrinite macerals.The correlation below of vitrinite reflectance to Tmax is derived from Barnett Shale samples:

$$Ro = 0.0180 * T\ max - 7.16$$

Mapping the thermal maturity of a shale play can aid in making drilling decisions. Gas can flow through low permeability rock such as shales better than oil, so drilling wells that target the formation where it has undergone paleotemperatures within the gas window often means better flow rates. Even within the gas window, there is a trend of increasing gas flow rates with increasing thermal maturity. Where low maturity Barnett shale is found, gas flow rates are lower (Jarvie et al., 2007). This is thought to be caused by the lower volumes of generated gas and the presence of residual hydrocarbon fluids that occlude the pore throats and reduce permeability. Figure 1-6 is a map of kerogen conversion based on HI generated from an extensive Barnett Shale core database (Jarvie et al., 2007). This map was found to correlate extremely well to thermal maturity. The study well of this report is located in southeast portion of Wise county in the most thermally mature part of the basin. Figure 1-7 shows the link between Barnett Shale vertical well production and thermal maturity (Jarvie et al., 2007). The TP Sims #2 study well would be expected to be one of the better gas producers in the field based on its thermal maturity.

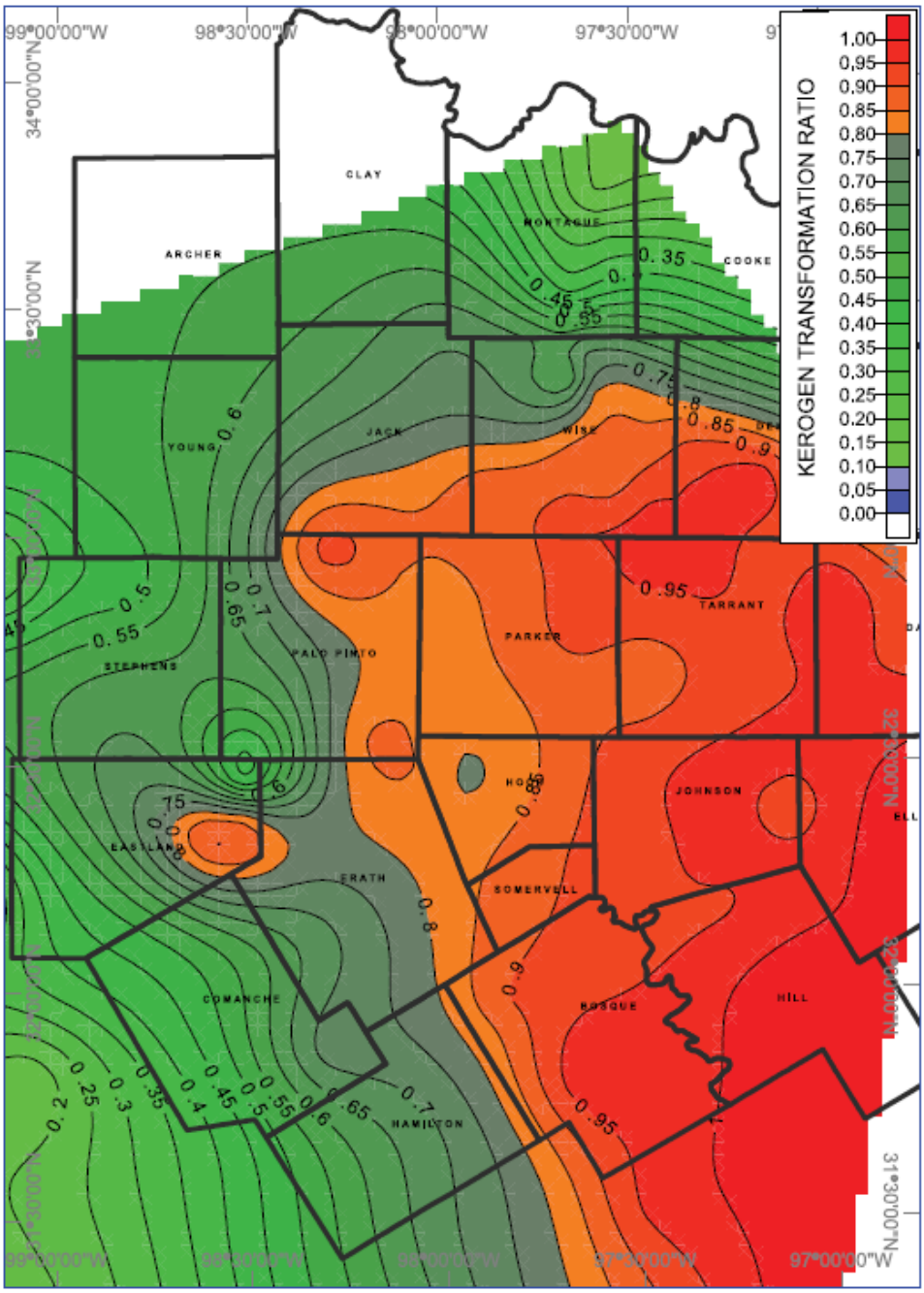

Figure 1-6 Kerogen transformation ratio map of Barnett Shale

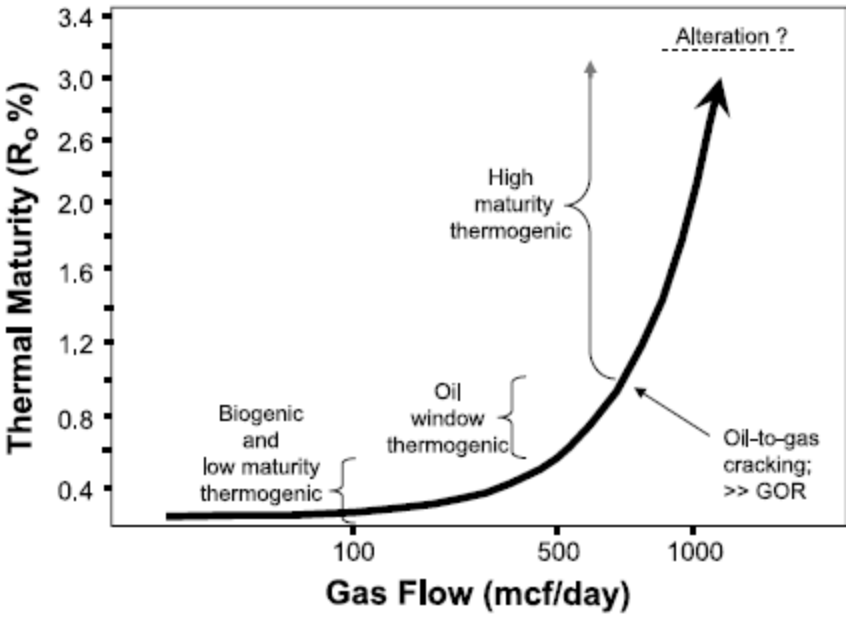

Figure 1-7 Correlation of thermal maturity to gas flow for Barnett Shale wells

Laboratory Adsorption

Gas adsorption is the accumulation of gas molecules on the surface of an adsorbent. Adsorption is described through isotherms where the amount of gas on the adsorbent is a function of its pressure at a constant temperature (Zhang et al., 2013). For unconventional gas resources, sorbed phase estimates are an important component of storage and transport calculations. In organic porous materials, gas can be stored as compressed fluid inside pores or it can fill up the micropores of solids (absorption) or remain outside the pores of solids attached to the pore walls of kerogen or clays (adsorption) (Santos and Akkutlu, 2013). Adsorption and absorption together are termed sorption.

Gas-in-place estimates for shale plays take into account both free and sorbed natural gas components. Organic-rich shales have larger methane-sorption capacity than clay-rich rocks lacking organic matter (Zhang et al., 2013). Variations in sorption capacity can be related to the difference in gas composition, clay type and abundance, moisture content, kerogen type, total organic carbon, and thermal maturity. Overall sorption capacity is proportional to surface area. The more sites available for gas to adsorb onto, the more gas will adsorb.

The sorbed gas volume is often quantified through the use of Langmuir isotherm. The sorption isotherm relates the sorbed-gas storage capacity of a porous material to the pore pressure. The most commonly used Langmuir model is a nonlinear relationship between the amount of gas sorption by the solid matrix and the pore pressure (Santos and Akkutlu 2013):

$$G_S = G_{SL}*(P/P+P_L)$$

G_S is sorbed-gas storage capacity (scf/ton)

P is pore pressure (psi)

G_{SL} is Languir volume (scf/ton)

P_L is Langmuir Pressure (psi)

The Langmuir volume represents the maximum amount of sorbed gas by solids when all available macromolecular sites and pore walls are taken by gas molecules. The Langmuir pressure is the pore pressure at which half of that maximum storage capacity is obtained. Langmuir volume will tend to increase with an increasing organic solid volume.

Langmuir isotherms from Lower Barnett samples for T.P. Sims #2 have been interpreted to indicate that for the adsorption sites are saturated at 1000 psi and above (Lancaster et al., 1992). Above 1000 psia, gas storage occurs primarily in the free porosity. Below 1000 psia, the gas desorption therefore plays a larger role (Lancaster et al., 1992). Since Barnett Shale reservoir pressures are approximately 3500 to 4000 psia, the reservoir has been predicted to behave similar to a traditional reservoir with regard to reservoir pressure and production behavior and below 1000 psi gas recovery from gas desorption will play a greater role (Lancaster et al., 1992).

Natural Fractures and Maximum Stress Direction

Past and current maximum stress directions help determine the optimal orientation for horizontal drilling. Acting as planes of weakness, natural fractures can be reactivated during well stimulation and enhance the production efficiency by widening the hydraulic fracture treatment zone (Gale et al., 2007). Stress directions can be deduced from wellbore breakouts or drilling-induced fractures on image logs. Core analysis of orientation, size and sealing properties can be

used to understand fracture pattern development. 3D seismic data can be used to map fault and fracture trends. Seismic mapping of connectivity to underlying water-bearing karsts, such as the Ellenburger formation, can help avoid drilling these areas. Once the maximum stress direction is determined, lateral orientation perpendicular to maximum stress direction will optimize transverse fracturing.

Two sets of natural fractures patterns have been identified for Fort Worth Basin: an older north-south trending set and a younger west-northwest—east-southeast set (Gale et al., 2007). Most natural fractures in Barnett Shale are sealed. The present-day maximum horizontal stress direction of Fort Worth Basin is northeast-southwest. To maximize hydraulic fracture propagation, most horizontal Barnett Shale wells are drilled perpendicular to the maximum stress direction in northwest-southeast directions. Figure 1-8 shows the TP Sims #2, API 33586 and the nearby wells from data obtained by the Texas Railroad Commission on June 4, 2014.

Figure 1-8 Drilling path of TP Sims #2 and nearby wells.

Chapter 2

Methodology

Study Question

The main objective of this study is to determine if well log and core-derived estimates of petrophysical properties can be used to generate meaningful original gas-in-place volumes that correlate with field performance in unconventional reservoirs. Moreover, key petrophysical modeling steps when evaluating source rock plays are examined.

While there is a large amount of current research on shale source rocks, there remains a void in the literature that links geology, engineering, and petrophysics. Past studies have shown widely varying estimates of original gas-in-place for the Barnett Shale from 13.3 bcf/Section (GRI 1991) to 204 bcf/Section and (Jarvie et al., 2007). For this study, well performance-based estimates of OGIP will be compared to estimates derived from rigorous petrophysical modeling.

Petrophysical Modeling of Barnett Shale

Digital well log data for Thomas P Sims #2 were imported into Schlumberger's petrophysical software Techlog to be used for well log-derived estimates of mineralogy, gross and net reservoir thickness, porosity, and water saturation. Core measurements from TP Sims #2 and other published sources were used to verify and calibrate the well log interpretation of each of these key petrophysical properties.

Mineralogy

The first step is to identify mineral components within the reservoir. Typical mineral constituents of shale source rocks include pyrite, quartz, calcite, dolomite and clay minerals such as illite-smectite and kaolinite. Core-derived X-ray diffraction data provide calibration points for mineral volume modeling. Approximate mineral volumes of major minerals present were quantified using well log analysis techniques. Because clay-rich intervals have the lowest permeability, and clay minerals exist in large proportion in Barnett Shale, total clay volume was estimated. For the purposes of this study, clay volume and shale volume will be used interchangeably. Quartz and carbonate-rich intervals typically exhibit better well fraccability and

performance. Their brittleness allows for hydraulically-induced fractures to remain open. Quartz and carbonate volume estimates are collectively termed matrix. Pyrite is also commonly found in organic-rich shale intervals because of the reducing conditions that enhance organic matter preservation. Pyrite has the largest grain density of the minerals present in the Barnett Shale. Pyrite density is 5 g/cc, which is double most other sedimentary minerals in the rock. When found in large quantities, pyrite can have significant effects on the bulk density log. Often, pyrite volume can be correlated to TOC volume (Witkowsky et al., 2012). The relative volumes of pyrite, clay, and matrix minerals of Barnett Shale were estimated from TP Sims #2 and their respective grain densities were then combined using a general mixing law to approximate a total rock grain density.

Porosity

Identifying hydrocarbon-filled porosity from well logs is attainable when the constituents of the formation and their relative abundance are known. Total porosity is estimated from the bulk density well log and compared to neutron porosity and acoustic log porosity estimates. The mineral volumes described above are used to calculate a total rock grain density. A general linear mixing rule that combines the mineral volumes and their individual densities can be used to obtain the rock grain density.

The resulting estimate of total grain density can be used in conjunction with the bulk density log to obtain total porosity. Two total porosity estimates were obtained based on two drilling fluid invasion assumptions. The low-side porosity estimate (PHIT_LS) is based on a fluid density of 1 g/cc which is based on the assumption that the near well bore environment has been invaded by drilling fluid. Alternatively, if drilling fluid has not invaded the well bore when the bulk density is logged (because of low rock permeability), gas could be the fluid-filling the near well bore environment. The high-side porosity is based on this alternative assumption with a gas fluid density of 0.2 g/cc. The equation for both porosity estimates is below:

$$PHIT_{LS} = \frac{RHOMA - RHOB}{RHOMA - 0.2}$$

$$PHIT_{HS} = \frac{RHOMA - RHOB}{RHOMA - 1}$$

Water Saturation

Most well log-derived water saturation estimates are derived from Archie's law which relates conductivity of a clean, consolidated sandstone rock to its porosity and water saturation (Archie, 1950). Archie's law is a purely empirical formula that describes ion flow through sandstones with varying intergranular porosity. Archie's law is describe as follows:

$$Sw = \frac{Rw}{Rt * \Phi^m}^{1/2}$$

Where

Sw is water saturation (decimal)

Rt is true resistivity (log-reading) (ohm.m)

Φ is porosity (v/v)

m is cementation exponent

Rw is formation water resistivity (ohm.m)

An underlying assumption for Archie's law is that there is a continuous conductive pathway of ion-filled formation water within the pore spaces of the rock. Rock and hydrocarbon fluids are resistive to electric conduction, while ion-filled water is an electrical conductor. When porosity, formation water salinity, in-situ resistivity, and rock tortuosity are known, the relative amount of ion-filled water can be estimated and hydrocarbon saturation can be determined. Barnett Shale has been demonstrated to be water-wet (Zhao et al., 2007). This means there is likely a continuous pathway, but that pathway is likely more tortuous than in typical sandstone rocks. As of yet, there is no known empirical derivation of water saturation from electric well logs using shale source rock samples.

Variations of Archies water saturation equation for shaley sands are based on effective porosity, which for shale samples is difficult to attain. This study focuses on total porosity, with no attempt on estimating effective porosity. Therefore, the water saturation estimate needs to be

based on total porosity as well. For this study, water saturation from well logs will be estimated with the Archie's model since it is based on total porosity. Formation water salinity is likely salt-saturated (Zhao et al., 2007) so the corresponding water resistivity at formation temperature, Rw, used in the study is 0.03 ohm.m. Cementation exponent, m, is approximately 2 as evidenced by formation factor study of mudstones (Zhao et al., 2007).

Net Pay

Gross thickness of Lower Barnett Shale formation is calculated from the top and base of the shale interval on the logs. Net thickness is computed as the gross thickness less non-reservoir rock thickness. Identifying non-reservoir rock in shale source rock plays is difficult because knowing the type of rock that contains moveable gas that can contribute to production is not entirely understood. For conventional reservoirs, cutoff criteria, often defined by core analysis of porosity and permeability, can be used. However, typical permeability cutoffs would eliminate all reservoir rock in unconventional reservoirs.

For this study, a range in net reservoir rock that contains moveable gas volumes will be found by applying varying porosity cutoff criteria. Petrophysical averages were calculated using the following porosity cutoffs: 0%, 0.1%, 1%, 2%, 4%, and 6%. Intervals with less than the porosity cutoff are excluded from net pay.

Permeability

Permeability of shales is typically in the nano-Darcy range for the shale matrix. Higher permeability rocks have a higher flow capacity and therefore better oil and gas flow rates. Permeability and porosity generally have a positive correlation such that increasing porosity means great permeability. No permeability estimates from core measurements were available for TP Sims #2. However, permeability can also be obtained from reservoir engineering analysis of well flow performance. Estimates of 1-2 md ft have been made from Lower Barnett Shale which on average came out to be 0.0054 mD (Lancaster et al., 1992). This likely includes the contribution of microcracks. The pre-fracture and post-fracture well test analyses indicated that a single layer model was insufficient to describe the flow behavior and fracture length (Lancaster et

al., 1992). Barnett Shale has a complex permeability distribution and cutoffs can be used to define units for a dual layer flow model that matches well performance data. Results have indicated that a good match can be obtained modeling the Barnett Shale with a higher permeability layer corresponding to an 8% porosity cutoff and 0.0025 mD, and a lower permeability layer (5% porosity cutoff) of 0.00015 mD (Lancaster et al., 1992).

Sorbed Gas Content

Primary storage of gas within Barnett shale is both within rock matrix and kerogen pore spaces. For shale reservoir, gas is typically partitioned between sorbed and free gas. Adsorbed gas is estimated using Langmuir isotherms and total gas volume calculated by summing the free and adsorbed gas content. Typical pressure and temperature data of Barnett Shale wells are used in conjuction with published Langmuir data to calculate the amount of adsorbed gas.

Volumetrics

Volumetric estimates of OGIP can be calculated using the following formula (Craft and Hawkins):

OGIP = 43,560 A*H*Φ*(1-Sw)/Bg

Where:

A is area (acres)

H is net formation thickness (ft)

Φ is porosity (decimal)

Sw is water saturation (decimal)

Bg is gas volume factor

Area

For the purposes of this study, OGIP will be reported in bcf/section as this is a common measure of OGIP for shale plays in the US. There are 640 acres/section and 43,560 square feet per acre.

Gas Expansion Factor

Gas volume expansion occurs as gas is brought from subsurface temperature and pressure conditions to surface conditions. The volumetric expansion of gas factor, Bg, is used to

relate the volume obtained at the surface to the volume of fluid actually occupied when it is compressed in the reservoir (Craft and Hawkins). The gas volume expansion factor can be estimated using the following formula:

$$Bg = 0.02829*(ZT/P) \text{ cu ft/SCF}$$

Where

Bg= gas volume factor (cu ft/SCF)

Z = gas compressibility factor

P= reservoir pressure (psi)

T= reservoir temperature (deg Rankine)

The Barnett Shale is normally pressured, and formation pressure is estimated at TP Sims #2 location to be approximately 4000 psi and the formation temperature is approximately 200 degF or 660 Rankine (Lancaster et al., 1992).

Well Performance

Over 20 years of Barnett Shale gas production data from the vertical study well has been obtained from DrillingInfo. The production data was fit using hyperbolic decline as shown in Figure 2-1. Production data ranges from April 1991 through September 2014 and cumulative gas production for this wellbore is 2.55 bcf. Spikes in production correspond to restimulation efforts (Jarvie et al., 2007). The EUR estimates from decline curve analysis are approximately 2.75 bcf. This estimate of EUR will be used for determining recovery factor for the range of volumetric OGIP.

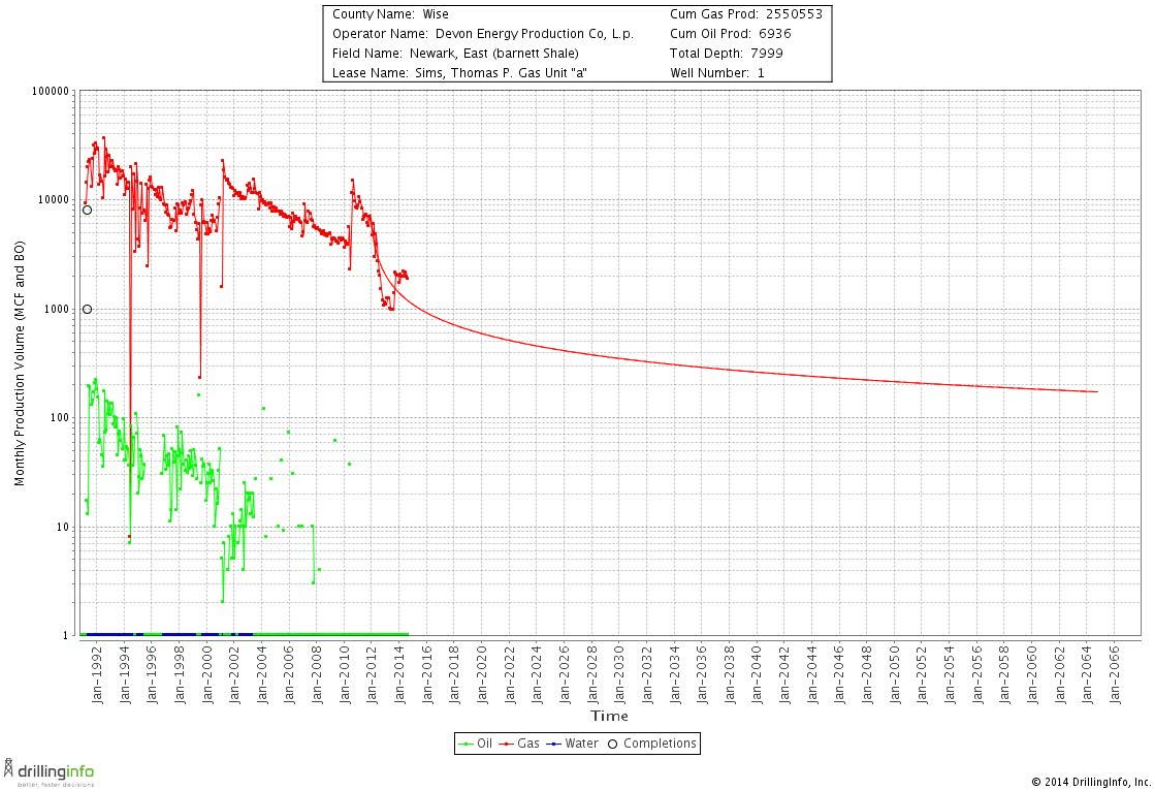

Figure 2-1 TP Sims production history and EUR

Chapter 3

Results

Well log and Core-Derived Properties

Clay volume estimates were derived using neutron and density logs of TP Sims #2 through the implementation of industry standard equation in Figure 3-1. Shale parameters displayed in Table 3-1 were selected such that average log-derived estimates of clay volume are consistent with published average clay volume from XRD. Figure 3-2 shows the statistics of the log-derived average clay volume. The arithmetically averaged clay volume over the Lower Barnett Shale interval is 36%. This is in agreement with reported XRD clay volumes of Lower Barnett Shale of 34% (Lancaster et al., 1992).

$$Vshale = \frac{(X1 - X0)}{(X2 - X0)} \quad \text{with}$$

$$X0 = NPHI_{MA}$$
$$X1 = NPHI + M1 \times (RHOB_{MA} - RHOB)$$
$$X2 = NPHI_{Sh} + M1 \times (RHOB_{MA} - RHOB_{Sh})$$
$$M1 = \frac{NPHI_{FL} - NPHI_{MA}}{RHO_{FL} - RHOB_{MA}}$$

Figure 3-1 Techlog shale volume formula

Table 3-1 Neutron and bulk density parameters

Name	Abbreviation	Unit	Description	Value
Neutron porosity	NPHI	v/v	Neutron porosity log reading in zone of interest	NPHI
Bulk density	RHOB	g/cm3	Bulk density log reading in zone of interest	RHOB
Neutron Porosity Matrix	$NPHI_{MA}$	v/v	Neutron porosity log reading in 100% matrix rock	0.00
Neutron Porosity Shale	$NPHI_{SH}$	v/v	Neutron porosity log reading in 100% shale	0.40
Neutron Porosity Fluid	$NPHI_{FL}$	v/v	Neutron porosity log reading in 100% water	1.00
Bulk Density Matrix	$RHOB_{MA}$	g/cm3	Bulk density log reading in 100% matrix rock	2.68
Bulk Density Shale	$RHOB_{SH}$	g/cm3	Bulk density log reading in 100% shale	2.45
Bulk Density Fluid	RHO_{FL}	g/cm3	Bulk density log reading in 100% water	1.00

Well	42497335860000
Dataset	RAW
Zone	Lower Barnett Shale
Variable	VSH_ND
Unit	v/v
Number of values	610
Minimum	0
Maximum	1
Arithmetic mean	0.3617218
Geometric mean	0.3331753
Harmonic mean	0.2525343
Third power	0.316015
Median	0.3721813
Mode	0
Standard Deviation	0.1608934
Variance	0.0258867

Figure 3-2 Shale volume statistics for TP Sims #2

Core TOC measurements were correlated to gamma ray (GR) and bulk density (RHOB) logs. Both of these log-derived estimates of TOC returned similar averages. The GR-TOC estimates were selected to use for further modeling purposes. Figure 3-3 shows the GR to TOC correlation and Figure 3-4 shows the RHOB to TOC correlation. Statistics of both well log-derived

TOC estimates compared to core TOC measurements from Lower Barnett Shale of TP Sims #2 are shown in Figure 3-5.

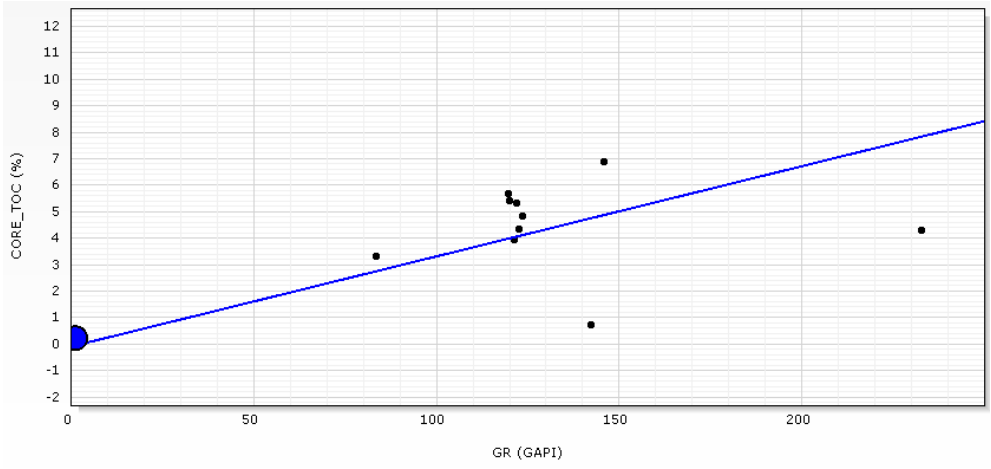

Figure 3-3 Gamma ray correlation to core TOC measurements

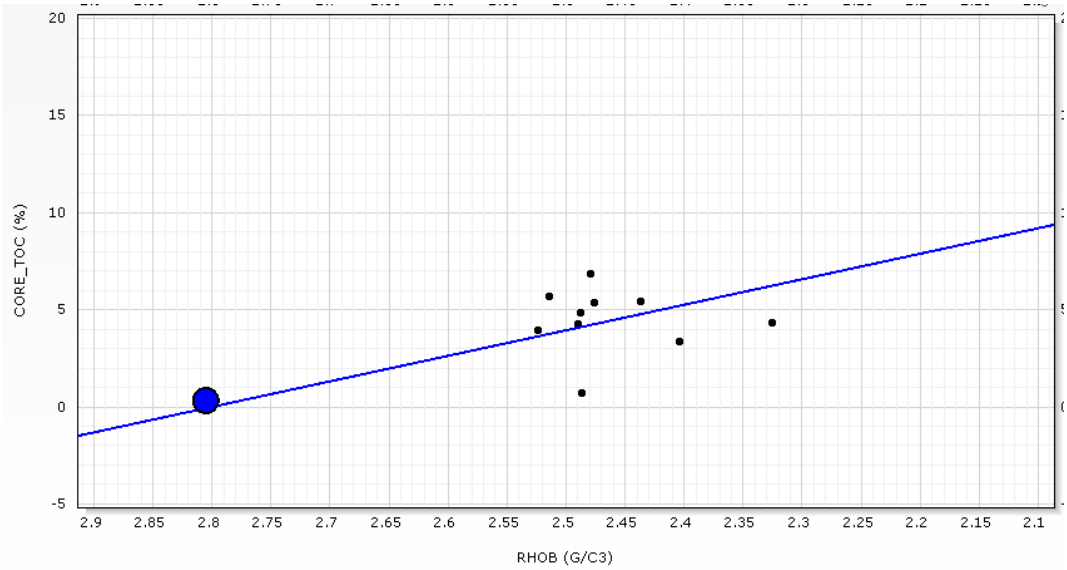

Figure 3-4 Bulk density correlation to core TOC measurements

Variable	TOC_RHOB_CL	TOC_GR_CL	CORE_TOC
Unit	v/v	v/v	
Number of values	610	610	10
Minimum	0	0.01430599	0.0071
Maximum	0.07859811	0.1012907	0.0685
Arithmetic mean	0.04040132	0.04728244	0.04453
Geometric mean	0.04000287	0.04548682	0.03940294
Harmonic mean	0.0384464	0.04391501	0.02996512
Third power	0.03877049	0.04605604	0.04153603
Median	0.04060701	0.04293729	0.0456
Mode	0.04060701	0.1011272	0.0071
Standard Deviation	0.009629942	0.01424055	0.01654059
Variance	9.27358e-05	0.0002027931	0.0002735912

Figure 3-5 Statistics of core TOC measurements and log-derived TOC estimates

Gas generation occurs when the weight percent of carbon in the kerogen is approximately 85-92% (Harwood, 1977). Therefore, the weight fraction of kerogen can be calculated from the well log-derived TOC weight fraction estimate as shown below:

$$WKER = WTOC / 0.90$$

where

WKER is the weight fraction of kerogen

WTOC is the weight fraction of TOC

To convert the weight fraction to volume fraction, the density must be known. The density of kerogen varies depending on kerogen type and thermal maturity. Ranges of kerogen density from approximately 1.1 to 1.4 g/cc have been estimated with the density increasing with increasing thermal maturity (Jizba, 1991). For the purposes of estimating kerogen volume, the kerogen density was assumed to be 1.2 g/cc and the volume fraction of kerogen was estimated using the following formula (Edmunson & Raymer, 1979):

$$VKER = (WKER / \rho_{ker}) * \rho$$

where

VKER is the volumetric fraction of kerogen in a mixture

WKER is the weight fraction of kerogen in a mixture

ρ_{ker} is the density of kerogen, g/cc

ρ is the bulk density of the mixture (RHOB well log), g/cc

Published XRD and TOC data for W.C. Young No. 2 well in Wise County was used for building a correlation of pyrite to TOC (Jarvie et al., 2005). This correlation, shown in Figure 3-6, was used for making estimates of pyrite in the TP Sims #2 well log interpretation. The log-derived TOC estimates were used to generate the pyrite estimate for each half foot sample over the Lower Barnett shale for TP Sims #2. The pyrite weight fraction (WPYR) was converted to pyrite volume fraction (VPYR) using the same relationship previously described for kerogen. The resulting pyrite volume was limited to values between 0 and 1.

VPYR = WPYR*RHOB/5

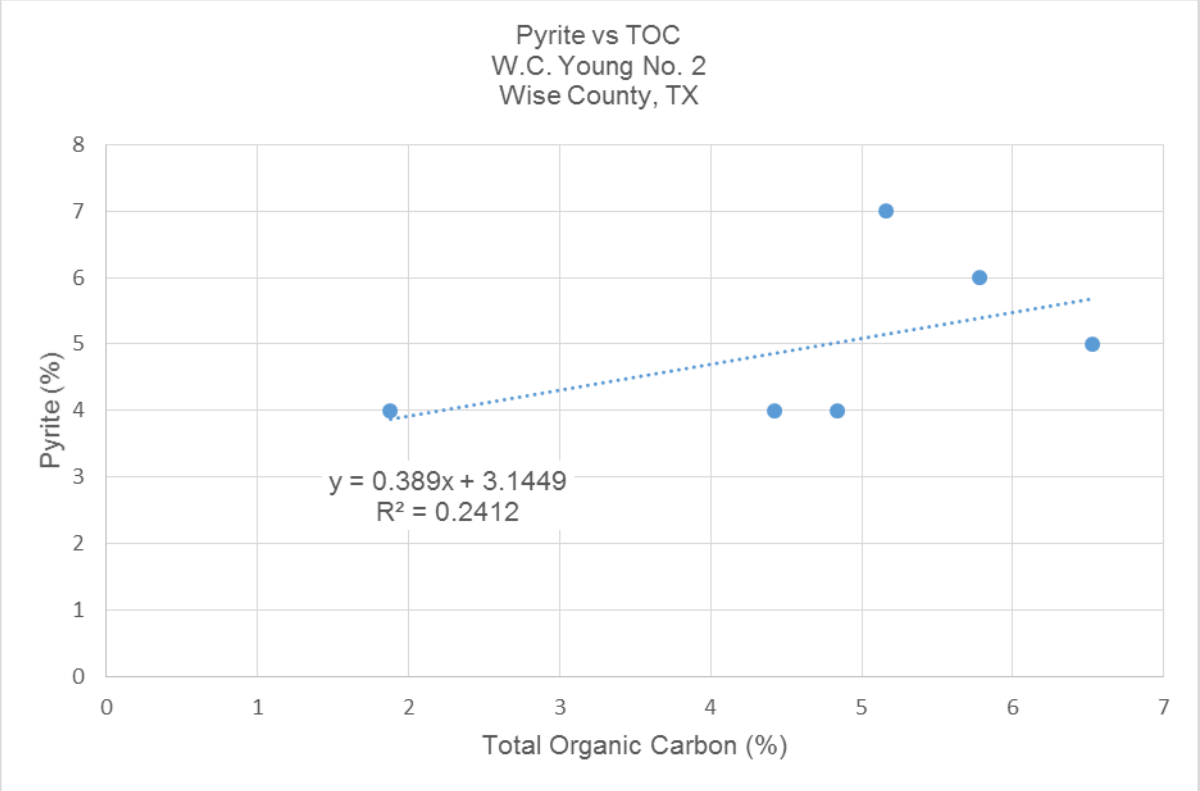

Figure 3-6 Pyrite to TOC correlation from WC Young 2 XRD data

After volumes of pyrite, shale, and TOC were computed, the remaining volume is predominantly quartz and carbonate grains. A grain density of 2.67 g/cc was assumed for this remaining mineral volume. Matrix density, (RHOMA), is used to define density of the entire rock

matrix composed of all minerals and organic content. The following equation is a linear mixing law that was used to calculate rock matrix density (RHOMA):

$$RHOMA = VSH\_ND*2.8 + (1-VSH\_ND-VPYR-VKER)*2.67+VKER*1.2 + VPYR*5$$

Well log-derived matrix densities were in agreement with the whole core grain density measurements (Figure 3-7).

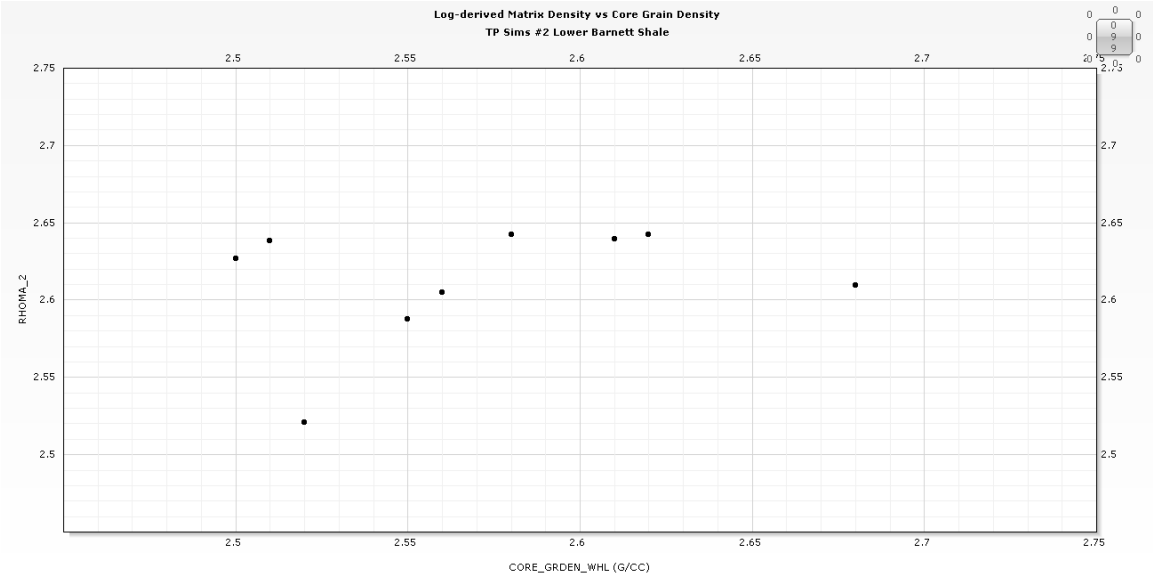

Figure 3-7 Comparison of log-derived grain density to core-derived grain density

Both the high side and low side well-log derived porosity estimates were within range of the core-derived porosity measurements. A crossplot of both high-side (black) and low-side (blue) well-log derived porosity versus whole core porosity is shown Figure 3-8. Figure 3-9 shows the same comparison of high-side (black) and low-side (blue) log-derived porosity to whole core porosity. The high and low well log-derived porosities differed by approximately 2 percent.

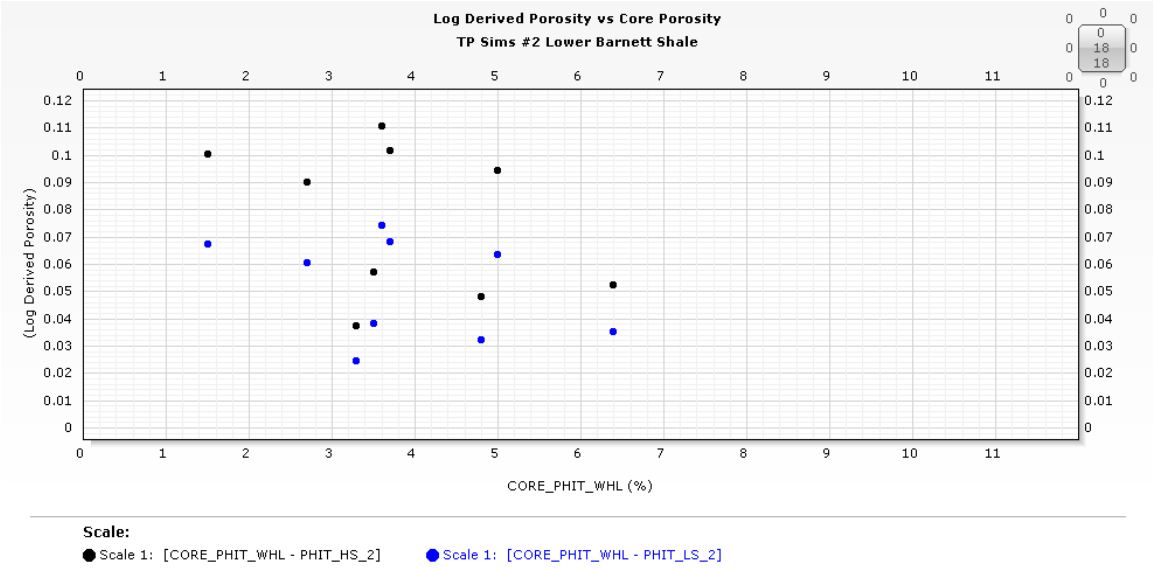

Figure 3-8 Crossplot of log-derived and whole core porosities

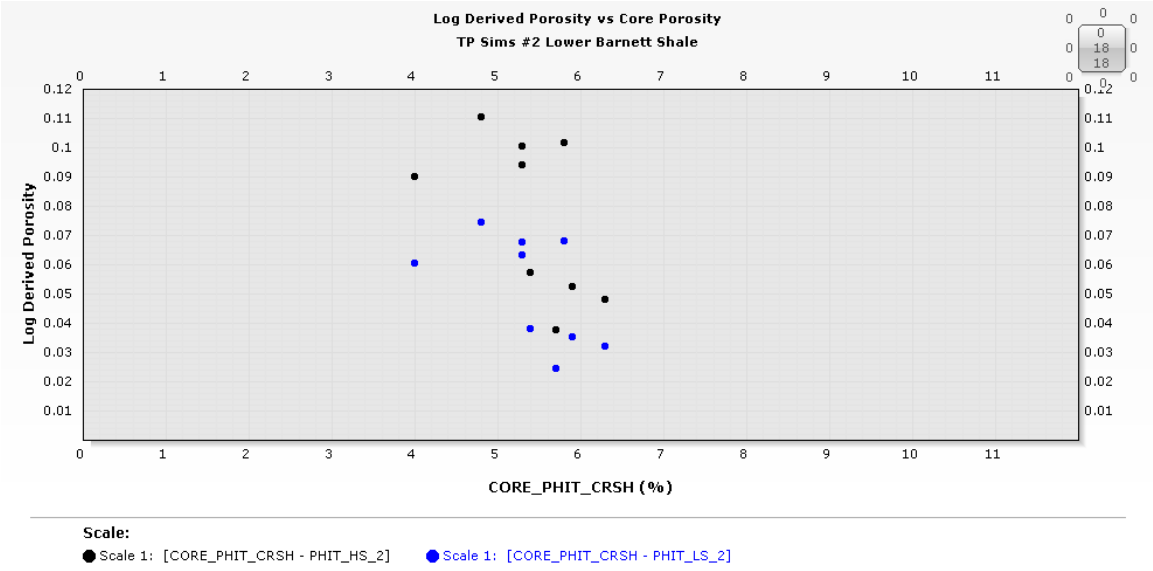

Figure 3-9 Crossplot of log-derived and crushed core porosities

Water saturations calculated from the high and low side porosity estimates ranged from a minimum of 3% to 100% in the Lower Barnett. The averages over the entire Lower Barnett shale

are displayed in Figure 3-10. The low side average water saturation is approximately 37% and the high side estimate average is 27%.

	1	2
Well	42497335860000	42497335860000
Dataset	RAW	RAW
Zone	Lower Barnett Shale	Lower Barnett Shale
Variable	SW_AR_HS_2	SW_AR_LS_2
Unit	v/v	v/v
Number of values	610	610
Minimum	0.03522179	0.05287427
Maximum	1	1
Arithmetic mean	0.2711523	0.3729627
Geometric mean	0.211872	0.3083141
Harmonic mean	0.1740559	0.2585961
Third power	0.2287145	0.3281498
Median	0.1924504	0.2866044
Mode	1	1
Standard Deviation	0.2287231	0.2494642
Variance	0.05231424	0.06223239

Figure 3-10 Statistics of water saturation estimates from low and high side cases

The detailed petrophysical well log display of TP Sims #2 showing the interpreted well log results and core measurements is shown below in Figure 3-11.

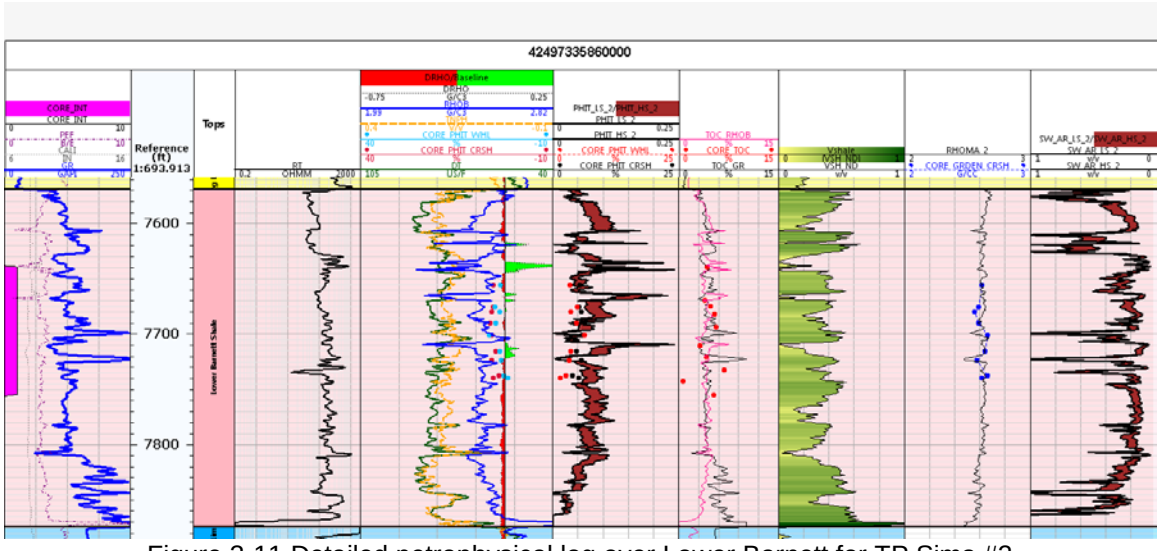

Figure 3-11 Detailed petrophysical log over Lower Barnett for TP Sims #2

Table 3-2 displays the high and low side petrophysical averages over the Lower Barnett interval with the range of cutoff criteria applied. Net pay for the various porosity cutoffs range from as low as 120 feet to 305 feet. Average porosity range from 5 to 10% and water saturations range from 14 to 28%.

Table 3-2 Interpreted petrophysical properties for TP Sims #2 for varying cutoffs

Petrophysical Sensitivity Results of TP Sims #2 Well Log Interpretation												
Lower Barnett Shale												
				Low Side				High Side				
			Gross		Average	Average	Average Water		Average	Average	Average Water	
	Top	Base	Interval	Net Pay	Vshale	Porosity	Saturation	Net Pay	Vshale	Porosity	Saturation	
Cutoff Criteria	(ft)	(ft)	(ft)	(ft)	(dec)	(dec)	(dec)	(ft)	(dec)	(dec)	(dec)	
None	7569	7874	305	305	0.36	0.05	0.24	305	0.36	0.07	0.14	
Phit > 0.001	7569	7874	305	293	0.35	0.06	0.28	293	0.35	0.08	0.19	
Phit > 0.01	7569	7874	305	287	0.35	0.06	0.28	289	0.35	0.08	0.19	
Phit > 0.02	7569	7874	305	276	0.34	0.06	0.27	286	0.35	0.08	0.19	
Phit > 0.04	7569	7874	305	211	0.31	0.07	0.24	257	0.34	0.09	0.18	
Phit > 0.06	7569	7874	305	120	0.25	0.08	0.20	211	0.31	0.10	0.16	

Hydrocarbon pore thicknesses were calculated for each cutoff sensitivity. Table 3-3 shows the results for each cutoff case and Figure 3-12 shows a histogram of the results. Hydrocarbon pore volume thickness (HPVH) was calculated as follows:

HPVH = Porosity*(1-Water Saturation)*Net Pay

Table 3-3 Hydrocarbon pore volume thickness results for range of cutoffs

Hydrocarbon Pore Volume Thickness of TP Sims #2											
Lower Barnett Shale											
				Low Side				High Side			
			Gross		Average	Average Water			Average	Average Water	
	Top	Base	Interval	Net Pay	Porosity	Saturation	HPVH	Net Pay	Porosity	Saturation	HPVH
Cutoff Criteria	(ft)	(ft)	(ft)	(ft)	(dec)	(dec)	(ft)	(ft)	(dec)	(dec)	(ft)
None	7569	7874	305	305	0.05	0.24	11.64	305	0.07	0.14	19.39
Phit > 0.001	7569	7874	305	293	0.06	0.28	11.64	293	0.08	0.19	19.27
Phit > 0.01	7569	7874	305	287	0.06	0.28	11.62	289	0.08	0.19	19.50
Phit > 0.02	7569	7874	305	276	0.06	0.27	11.43	286	0.08	0.19	19.32
Phit > 0.04	7569	7874	305	211	0.07	0.24	10.48	257	0.09	0.18	18.87
Phit > 0.06	7569	7874	305	120	0.08	0.20	7.29	211	0.10	0.16	17.23

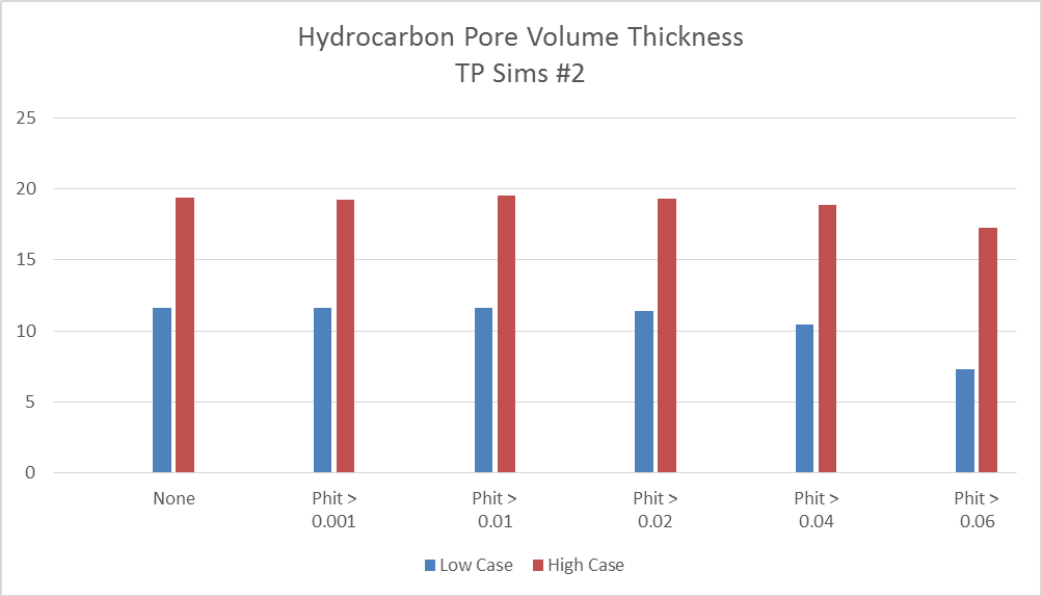

Figure 3-12 Hydrocarbon pore thicknesses for each porosity cutoff

Original Gas-in-Place

At 4000 psi and 200 degF, the Z factor is approximately 0.90. The gas expansion factor is found to be 0.0042 RCF/SCF.Table 3-4 shows the range of OGIP results in SCF/section, MMCF/section, and bcf/section for each set petrophysical properties as defined in Table 3-2 from well log interpretation. The range of OGIP based on each set of petrophysical properties interpreted from TP Sims #2 well logs is 48 to 129 bcf/section.

OGIP calculations are based on 55 acre spacing, and EUR of 2.75 bcf from the decline curve analysis of TP Sims #2. The EUR/section is approximately 32 bcf. Dividing the OGIP bcf/section by the wells/section, the range of OGIP/well is estimated to be 4.16 to 11.12 bcf. The ratio of EUR/well to OGIP/well is the recovery factor, which for these estimates ranges from 25% to 66%.

Table 3-4 OGIP, EUR, and RF estimates of Lower Barnett Shale

		Volumetric Estimates from Analysis of TP Sims #2											
		Low Side Results						High Side Results					
		None	Phit > 0.001	Phit > 0.01	Phit > 0.02	Phit > 0.04	Phit > 0.06	None	Phit > 0.001	Phit > 0.01	Phit > 0.02	Phit > 0.04	Phit > 0.06
Rock Properties	Porosity	5%	6%	6%	6%	7%	8%	7%	8%	8%	8%	9%	10%
	Water Saturation	24%	28%	28%	27%	24%	20%	14%	19%	19%	19%	18%	16%
	Avg Thickness (ft)	305	293	287	275.5	211	119.5	305	293	289	286	257	211
	Bulk Net Volume (Ac-ft)	195,200	187,520	183,680	176,320	135,040	76,480	195,200	187,520	184,960	183,040	164,480	135,040
OGIP	OGIP (MMCF/Sec)	77,215	77,210	77,111	75,864	69,534	48,396	128,657	127,884	129,412	128,226	125,223	114,360
	OGIP (BCF/Sec)	77	77	77	76	70	48	129	128	129	128	125	114
	TP Sims #2 EUR (BCF/well)	2.75											
	Acre Spacing	55.0											
	Wells /Section	11.6											
	EUR/Section	32.0											
	OGIP (BCF/Well)	6.64	6.64	6.63	6.52	5.98	4.16	11.06	10.99	11.12	11.02	10.76	9.83
Reovery Factor	EUR/OGIP	41%	41%	41%	42%	46%	66%	25%	25%	25%	25%	26%	28%

Chapter 4

Discussion

Mineral volumes, porosity, gross thickness, net thickness and water saturation of the Lower Barnett Shale were determined from well log interpretation of TP Sims #2 well of Wise County, TX. Typical industry standard log interpretation procedures were modified to account for shale source rock constituents including pyrite, TOC, and kerogen. The well log interpretation modeling work was calibrated to available core measurements of TOC, clay, and pyrite volume and porosity.

As is typical for shale plays, TOC correlated favorably to bulk density and to natural gamma radiation logs. Also, a positive correlation between the amount of pyrite and TOC worked well for obtaining pyrite volumes once the TOC estimate had been obtained from well logs. However, since these correlations are derived from limited core data, they should be reexamined as additional XRD measurements are made available. This method of using well logs to estimate TOC and pyrite can easily be applied to other marine shale source rocks where core data is available.

The results from the well log interpretation were used to generate a range of OGIP estimates. The range of OGIP was defined by variation of two parameters: cutoff criteria and the near-borehole fluid assumption for porosity calculations. The well log interpretation results indicate OGIP ranges from 49 to 129 bcf/section. These estimates are lower than estimates of OGIP from EUR (based on production profiles) that were found to be range from 151 to 291 bcf/section (Jarvie et al., 2007).

Typical EURs for Barnett Shale wells range from 1.75 to 3 bcf. The TP Sims #2 well is a vertical well in a better producing part of the field. Assuming 2.75 bcf as the EUR for this well, and 55 acre well spacing, recovery factors ranged from 25% to 66%. These recovery factors are higher than expected for shale source rock plays. Recovery factors for Barnett Shale wells are in the 8-12% range (Jarvie et al., 2007).

Conclusions

Poorer quality reservoir rocks typically have lower recovery factors. This is because less hydrocarbon can be produced from lower permeability reservoirs and remains trapped in the formation. The high recovery factors obtained from the results of this study suggests that the well log interpretation has not accounted for all of the OGIP for the Barnett Shale or that the well is connecting to a larger volume of rock than what is assumed in this study.

Hydraulic fracturing may affect the drainage area to a larger extent than what is modeled in this study. Additional work, potentially with microseismic data, can help identify the approximate drainage areas of hydraulically fractured Barnett Shale wells.

Methane gas has been shown to have the ability to adsorb onto organic matter and Langmuir adsorption curves can be used to approximate adsorbed gas content. The study here assumed that the wireline logs will be able to account for all gas (adsorbed and free). However, large amounts of adsorbed gas may affect the resistivity response and obstruct the continuous electrical conductive pathway necessary for the water saturation estimate to be accurate.

This study shows that there can be good agreement with log-derived and core-derived mineralogy and porosity. However, there still remains large uncertainty in the water saturation estimates from well log analysis. In particular, there is a lack of resistivity-based water saturation models designed specifically for shales. This remains a void for the oil and gas industry that has yet to be filled. Further research in this area will likely need to focus on correlating core-derived measurements of water saturation to resistivity-based estimates. Because shale source rock reservoirs have ultra-low permeability, laboratory Dean Stark apparatus may not be able to provide reliable measurements of water saturation. Research using high pressure capillary pressure techniques may be useful for gathering data to build an empirical resistivity-based model of water saturation.

Appendix A

Core Analysis Data

W. C. Young Core Data
Wise County, TX

Depth	Total Clay	Quartz	K Feldspar	Plagioclase	Calcite	Dolomite	Pyrite	Apatite	TOC
6090.5	16	10	0	0	55	17	2	0	
6920	35	44	1	2	4	7	4	3	4.84
6936	43	30	1	2	2	3	6	13	
6944	4	13	0	1	54	3	11	14	
6953.5	37	40	0	3	4	1	7	8	
6964	4	10	0	3	78	2	3	0	
6973	38	37	2	6	3	2	5	7	
6985	42	38	1	3	2	3	8	3	
7001	23	32	0	4	30	4	4	3	
7006	37	34	1	6	10	6	2	4	
7007	0	4	0	2	71	1	21	1	
7014	31	42	1	4	7	7	6	2	
7022.5	20	33	0	5	3	0	10	29	
7026	48	33	2	6	0	1	8	2	
7030.5	7	4	1	4	5	70	9	0	
7033	48	36	4	5	0	1	4	2	4.42
7045	37	40	2	4	2	8	5	2	
7061.6	41	42	2	3	3	3	5	1	
7065	45	40	1	4	0	2	6	2	
7075	37	43	1	4	3	3	6	3	
7081	18	17	0	4	2	55	4	0	1.88
7086	54	31	1	4	0	0	7	3	5.16
7095	46	34	0	4	0	5	9	2	
7108	32	31	3	4	2	20	6	2	5.78
7118	51	28	5	6	0	0	7	3	
7126	37	47	2	4	0	1	5	4	6.53
7135	48	33	3	5	0	3	7	1	
7141	45	34	1	3	3	4	6	4	
7150	50	34	2	4	0	0	8	2	
7156.5	21	23	1	2	42	3	4	4	

TP Sims #2 Core Data
Wise County, TX

	Whole Core		Crushed Core			
Depth	Porosity	Grain Density	Porosity	Grain Density	Depth	TOC
ft	%	g/cc	%	g/cc	ft	%
7,656	3.5	2.56	5.4	2.62	7640	4.33
7,676	5.0	2.58	5.3	2.59	7670	3.92
7,680	3.7	2.50	5.8	2.56	7675	4.79
7,690	4.8	2.55	6.3	2.59	7682	5.40
7,701	6.4	2.68	5.9	2.66	7694	5.66
7,716	3.6	2.61	4.8	2.64	7711	3.30
7,724	3.3	2.52	5.7	2.58	7721	4.26
7,738	2.7	2.62	4.0	2.66	7733	6.85
7,740	1.5	2.51	5.3	2.62	7743	0.71
					7755	5.31

References

Archie, Gustave Erdman. 1950. "Introduction to Petrophysics of Reservoir Rocks." AAPG Bulletin 34 (5): 943-961.

Browning, John, Svetlana Ikonnikova, Gurcan Gulen, and Scott Tinker. 2013. "Barnett Shale Production Outlook." . doi:10.2118/165585-PA.

Craft, B., C. and M. F. Hawkins. 1959. Applied Petroleum Reservoir Engineering. Englewood Cliffs, New Jersey: Prentice-Hall, Inc.

Edmundson, H. and Raymer, L.L. 1979. “Radioactive logging parameters for common minerals”. Log Analyst 20, 38-47.

Gale, Julia, Robert M. Reed, and Jon Holder. 2007. "Natural Fractures in the Barnett Shale and their Importance for Hydraulic Fracture Treatments." AAPG Bulletin 91 (4): 603-622.

Gas Research Institute. May 1991. Formation Evaluation Technology for Production Enhancement: Log, Core, and Geochemical Analyses in Barnett Shale, Mitchell Energy Corp., Thomas P. Sims no. 2, Wise County, Texas. Chicago, Illinois: Gas Research Institute.

Harwood, R. J. 1977. "Oil and Gas Generation by Laboratory Pyrolysis of Kerogen." *AAPG Bulletin* 61 (12): 2081-2102.

Hickey, James J. and Bo Henk. April 2007. "Lithofacies Summary of the Mississippian Barnett Shale, Mitchell 2 T.P. Sims Well, Wise County, Texas." AAPG Bulletin 91 (4): 437-443.

Jarvie, D. M., B. L. Claxton, F. Henk, and J. T. Breyer, 2001, Oil and shale gas from the Barnett Shale, Fort Worth Basin, Texas: AAPG Annual Meeting Program, v. 10, p. A100.

Jarvie, D. M., Ronald J. Jill, and Richard M. Pollastro. 2005. “Assessment of the Gas Potential and Yields from Shales: the Barnett Shale Model”, *in* Cardott, B.J. (ed.), Unconventional energy resources in the southern Midcontinent, 2004 symposium: Oklahoma Geological Survey Circular 110: 37-50.

Jarvie, Daniel M., Ronald J. Hill, Tim E. Ruble, and Richard M. Pollastro. April 2007. "Unconventional Shale-Gas Systems; the Mississippian Barnett Shale of North-Central Texas as One Model for Thermogenic Shale-Gas Assessment " (in Special Issue; Barnett Shale) AAPG Bulletin 91: 475-499.

Jarvie, D. M. “Unconventional Shale Resource Plays: Shale-Gas and Shale-Oil Opportunities.” Presentation at the Fort Worth Business Press Meeting, Fort Worth, TX, June 19, 2008.

Jizba, Diane Linda. 1991. *Mechanical and acoustical properties of sandstones and shales*. Thesis (Ph. D.)--Stanford University, 1991.

Lancaster, D. E., S. F. McKetta, R. E. Hill, F. K. Guidry, and J. E. Jochen. 1992. "Reservoir Evaluation, Completion Techniques, and Recent Results from Barnett Shael Development in the Fort Worth Basin." SPE Annual Technical Conference and Exhibition, Washington, D.C, Society of Petroleum Engineers, 4-7 October.

Loucks, Robert G. and Stephen C. Ruppel. 2007. "Mississippian Barnett Shale: Lithofacies and Depositional Setting of a Deep-Water Shale-Gas Succession in the Fort Worth Basin, Texas." AAPG Bulletin 91: 579-601.

Martineau, David. 2007. "History of the Newark East Field and the Barnett Shale as a Gas Reservoir." AAPG Bulletin 91: 399-405.

Miskimins, Jennifer. 2009. "The Importance of Geophysical and Petrophysical Data Integration for the Hydraulic Fracturing of Unconventional Reservoirs." (in Unconventional Resources and CO2 Monitoring) Leading Edge 28: 844-849.

Montgomery, S. L., D. M. Jarvie, K. A. Bowker, and R. M. Pollastro, 2005. “Mississippian Barnett Shale, Fort Worth basin, north-central Texas: Gas-shale play with multi-trillion cubic foot potential” AAPG Bulletin 89: 155-175.

Nicot, J. P., B. R. Scanlon, R. C. Reedy, and R. A. Costley. 2014. "Source and Fate of Hydraulic Fracturing Water in the Barnett Shale: A Historical Perspective." Environmental Science & Technology 48 (4): 2464-2471. doi:10.1021/es404050r [doi].

Pennslyvania Department of Conservation and Natural Resources. "Quality of Organic Matter.", accessed 11/5,2014,http://dcnr.state.pa.us/topogeo/econresource/oilandgas/marcellus/sourcerock_index/sourcerock_quality/index.htm.

Pollastro, Richard M. April 2007. "Total Petroleum System Assessment of Undiscovered Resources in the Giant Barnett Shale Continuous (Unconventional) Gas Accumulation, Fort Worth Basin, Texas." (in Special Issue; Barnett Shale) AAPG Bulletin 91: 551-578.

Pollastro, Richard M., Daniel M. Jarvie, Ronald J. Hill, and Craig W. Adams. 2007. "Geologic Framework of the Mississippian Barnett Shale, Barnett-Paleozoic Total Petroleum System, Bend arch–Fort Worth Basin, Texas." AAPG Bulletin 91: 405-436.

Santos Rueda, Jose Manuel and I. Y. Akkutlu. 2012. Laboratory Measurement of Sorption Isotherm Under Confining Stress with Pore Volume Effects Society of Petroleum Engineers. doi:10.2118/162595-MS.

Schmoker, James. 2002. "Resource-assessment perspectives for unconventional gas Systems." AAPG Bulletin 86: 1993-1999.

Slatt, Roger, Prerna Singh, Gariel Borges, Roderick Perez, Romina Portas, Julieta Vallejo, Mike Ammerman, and William Coffey. 2009. "Reservoir Characterization of Unconventional Gas Shales: Example from the Barnett Shale, Texas, U.S.A." AAPG Annual Convention, San Antonio, TX, Search and Discovery, April 20-23, 2008.

Texas A&M Ocean Drilling Program. "Rock Eval Pyrolysis.", accessed 11/5,2014, http://www-odp.tamu.edu/publications/tnotes/tn30/tn30_11.htm.

Tissot, B. P. and D. H. Welte. 1978. Petroleum Formation and Occurrence A New Approach to Oil and Gas Exploration. Germany: Springer-Verlag.

Witkowsky, Jim, James Glaford, John Quirein, and Jerome Truax. 2012. "Predicting Pyrite and Total Organic Carbon from Well Logs for Enhancing Reservoir Interpretation." Lexington, Kentucky, USA, SPE, October 3-5.

Zhang, Tonwei, Geoffrey E. Ellis, Stephen C. Ruppel, Kitty Milliken, Mike Lewan, and Xun Sun. 2013. Effect of Organic Matter Properties, Clay Mineral Type and Thermal Maturity on Gas Adsorption in Organic-Rich Shale Systems Society of Petroleum Engineers. doi:10.1190/URTEC2013-205.

Zhao, Hank, Natalie B. Givens, and Brad Curtis. April 2007. "Thermal Maturity of the Barnett Shale Determined from Well-Log Analysis." AAPG Bulletin 91: 535-549.

Biographical Information

Melanie Ybarra received her Bachelors of Science degree in mathematics with chemistry minor from University of Houston. She began her career as a petrophysical analyst at Netherland, Sewell, and Associates of Dallas, TX in 2005 with a team of petrophysicists working closely with petroleum engineers and geologists. She entered the petroleum geology program at University of Texas at Arlington in the fall of 2011. Her current interests include formation evaluation and reservoir characterization.